

## Supporting Information

### A high-sensitivity long-lifetime phosphorescent RIE additive to probe free volume-related phenomena in polymers

Valentina Antonia Dini, Alessandro Gradone, Marco Villa, Marc Gingras, Maria Letizia Focarete, Paola Ceroni, Chiara Gualandi, Giacomo Bergamini

#### 1. Experimental part

##### Materials

Polystyrene (PS,  $M_w = 30.5 \times 10^4 \text{ g mol}^{-1}$ , Carlo Erba), Polyvinyl acetate (PVAc,  $M_w = 50 \times 10^4 \text{ g mol}^{-1}$ , Sigma Aldrich), and Poly(L-lactide) (PLA,  $M_w = 8.4 \times 10^4 \text{ g mol}^{-1}$ , PDI = 1.7, Lacea H.100-E) were used. Tetrahydrofuran (THF,  $\geq 99.8\%$  Sigma Aldrich) and dichloromethane (DCM,  $\geq 99.8\%$  Sigma Aldrich) were used without further purification. Hexakis(4-methyl-1-phenylthio)benzene (A6Me) is the AIE probe used to dope the polymeric films and was synthesized as previously reported [1]. Table S1 summarize the photophysical behaviour of A6Me dye.

**Table S1. Photophysical data of hexakis(4-methyl-1-phenylthio)benzene (A6Me) under different experimental conditions [1].**

Absorption in $\text{CH}_2\text{Cl}_2$ , 298 K		Emission in solid phase, 298 K		
$\lambda^a$ [nm]	$\epsilon^b$ [ $\text{M}^{-1} \text{cm}^{-1}$ ]	$\lambda_{\text{max}}$ [nm]	$\tau^c$ [ $\mu\text{s}$ ]	$\Phi^d$
326	19200	510	3.0	1.0

<sup>a</sup>wavelength. <sup>b</sup>molar absorption coefficient. <sup>c</sup>lifetime. <sup>d</sup>photoluminescence quantum yield.

##### Film preparation

Homogeneous polymeric solutions were prepared by dissolving each polymer in the proper solvent (DCM in case of PLA and PVAc, THF in case of PS) at a concentration of 4% w v<sup>-1</sup>. A6Me was added to gain a final concentration of 2 wt% in the dry film. After stirring until complete polymer

dissolution, each mixture (50 ml) was gently poured into a glass petri dish ( $d = 7.5\text{mm}$ ) and left under the fume hood for solvent evaporation. In order to completely eliminate the solvent, the obtained films were separated from the petri, hot-pressed at a temperature of  $T_g+100^\circ\text{C}$  and rapidly cooled to room temperature.

Unaged samples were obtained by keeping the films at a temperature  $T=T_g+50^\circ\text{C}$  for 10 minutes to erase all prior thermal history, then rapidly quenched in liquid nitrogen and kept at  $-20^\circ\text{C}$  before analysis.

#### *Accelerated physical ageing experiments*

Physical ageing was induced by keeping the unaged films at about  $10^\circ\text{C}$  below their respective  $T_g$ : the annealing  $T$  ( $T_a$ ) was  $35^\circ\text{C}$  for PVAc,  $45^\circ\text{C}$  for PLA and  $90^\circ\text{C}$  for PS. The samples were maintained at this temperature for a certain ageing time ( $t_a$ ).

#### *Characterization methods*

Differential Scanning Calorimetry (DSC) was carried out using a Q2000 DSC apparatus (TA instruments) equipped with a Refrigerated Cooling System (RCS90). Samples were subjected to a first heating scan in the temperature range  $-90$ - $200^\circ\text{C}$  at a rate of  $20^\circ\text{C min}^{-1}$ , followed by a fast cooling to  $-90^\circ\text{C}$  and a second heating scan at  $20^\circ\text{C min}^{-1}$  to  $200^\circ\text{C}$ . The glass transition temperature ( $T_g$ ) was taken at half-height of the glass transition heat capacity step, while the crystallization temperature ( $T_c$ ) and the melting temperature ( $T_m$ ) were taken at the peak maximum of crystallization exotherm and melting endotherm, respectively.

Temperature Modulated DSC (TMDSC) was also performed from  $-90^\circ\text{C}$  to  $200^\circ\text{C}$ . The heating rate was  $3^\circ\text{C min}^{-1}$ , the modulation amplitude was  $0.477^\circ\text{C}$  and the oscillation period was 60 s. The enthalpic recovery of the aged samples was calculated as the area of the endothermal relaxation peak in the non-reversing heat flow signal, by following a previously reported method [2]. For a more accurate measure of the enthalpic recovery, after heating, the samples were cooled at  $3^\circ\text{C min}^{-1}$  and the exothermal peak area in the non-reversing signal, resulting from the so-called "frequency effect", was subtracted to gain the enthalpy of relaxation ( $\Delta H_{\text{relax}}$ ).

Photophysical measurements in solution were carried out in dichloromethane at 298 K. Luminescence measurements were performed on solid state samples. UV-vis absorption spectra were recorded with a PerkinElmer 140 spectrophotometer using quartz cells with a path length of 1.0 cm. Emission spectra were obtained with a Perkin Elmer LS55 spectrofluorometer.

Lifetimes shorter than 10  $\mu$ s were measured by an Edinburgh FLS920 spectrofluorimeter equipped with a TCC900 card for data acquisition in time-correlated single-photon counting experiments (0.5 ns time resolution) with a 405 nm laser.

Emission intensity decay measurements in the range 10  $\mu$ s to 1 s for external analysis (ageing and stress-strain tests) were performed on a homemade time-resolved phosphorimeter coupled with two optical fibres. The excitation source was a UV-LED centred at 365 nm while the detector was a conventional APD.

Emission quantum yield was calculated from corrected emission spectra registered by an Edinburgh FLS920 spectrofluorimeter equipped with a barium sulfate coated integrating sphere (4 in.), a 450W Xe lamp ( $\lambda$  excitation tunable by a monochromator supplied with the instrument) as light source, and a R928 photomultiplier tube, following the procedure described by De Mello et al. [3]. Radiative and non-radiative constants are calculated based on the following equations, with the assumption of unitary intersystem crossing efficiency and the absence of photoreactions.

$$\tau_{ph} = \frac{1}{k_r + k_{nr} + k_p} \quad \Phi_{ph} = \frac{\eta_{ISC} k_r}{k_r + k_{nr} + k_p} = \eta_{ISC} k_r \tau_{ph}$$

Where  $\tau_{ph}$  is the phosphorescence lifetime,  $\eta_{ISC}$  the efficiency of intersystem crossing between  $S_1$  and  $T_1$ ,  $k_r$  is the radiative rate constant,  $k_{nr}$  is the non-radiative rate constant and  $k_p$  is the photoreaction rate constant. The estimated experimental errors are: 2 nm on the absorption and emission band maximum, 5% on the molar absorption coefficient and shorter luminescence lifetime. In the case of longer lifetimes, the error is evaluated each time due to the external set-up (see below).

Stress-strain curves of A6Me doped films were recorded using an Instron Testing Machine 4465 and the Series IX software package. Dog-bone shaped specimens (gage length = 20 mm, width = 5 mm, thickness = 0.1-0.2 mm) cut from each film were tested in traction mode with a load cell of 100 N. The crosshead speed was set at 0.5 mm  $\text{min}^{-1}$  for PLA and PS and at 3 mm  $\text{min}^{-1}$  for PVAc. Load-displacement curves were acquired and converted to stress-strain curves. At least 4 specimens were tested for each polymer and mechanical data were provided as the average value  $\pm$  standard deviation.

## DSC analysis of polymeric films

Figure S1 reports the DSC curves of the pure polymeric films, and of the corresponding films loaded with A6Me to assess the possible effect of A6Me on polymer thermal transitions. For a reliable comparison, all samples have been subjected to a first heating followed by a fast cooling to erase polymer thermal history. The atactic polystyrene (Figure S1a) and the polyvinyl acetate (Figure S1b)

only show a heat capacity step at the expected glass transition temperature, 97 °C and 43 °C, respectively. Differently, the stereoregular PLA has the capability to partially crystallize. This is evident in the DSC scan, since, after the glass transition region, the polymer shows a cold crystallization exotherm peak followed by a melting endotherm peak of exactly the same entity ( $\Delta H_c = \Delta H_m = 45 \text{ J g}^{-1}$ ), meaning that the quenched PLA film is completely amorphous since the fast cooling prevents the polymer from crystallizing. The addition of 2 wt% of A6Me does not affect polymer  $T_g$  but the enthalpy of cold crystallization and the subsequent melting of the same entity are lower ( $\Delta H_c = \Delta H_m = 33 \text{ J g}^{-1}$ ), suggesting that A6Me reduces the polymer rate of crystallization. It is worth mentioning that also in the first heating scan PLA samples obtained after hot-pressing did not present any crystalline phase and were thus completely amorphous.

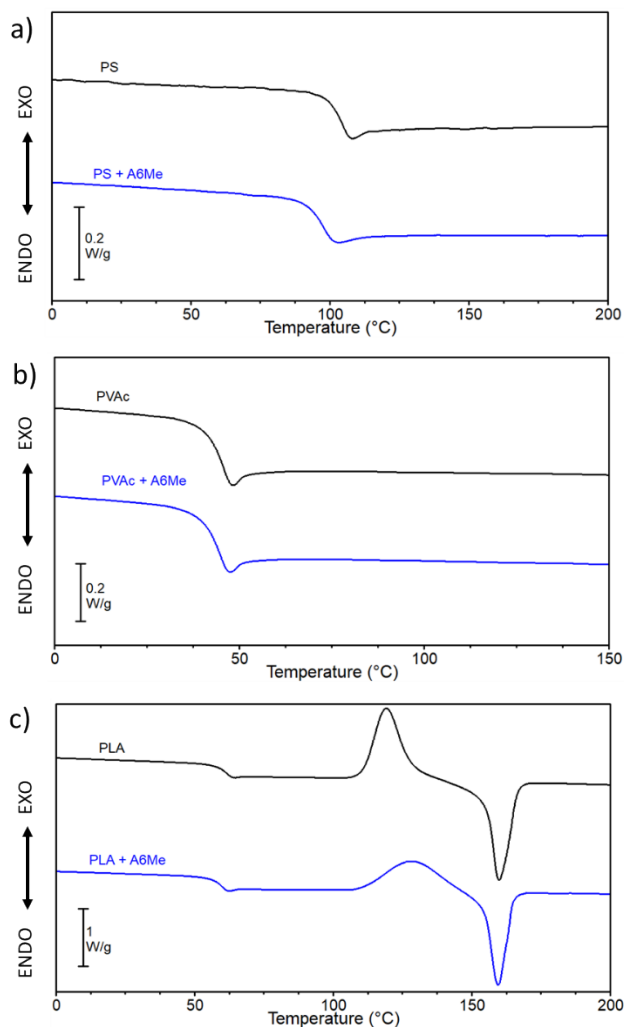


**Figure S1.** DSC 2<sup>nd</sup> heating curves of doped (blue) and undoped (black) films: PS (a); PVAc (b); PLA (c).

## Sample characterization after physical aging

MDSC analysis allows to separate the change of heat capacity occurring at  $T_g$  from the endothermic peak caused by the enthalpic relaxation process of physically aged samples. Figure S2 reports a representative MDSC analysis performed on an aged PVAc sample. The curves of the total heat flow (T), reversing heat flow (R) and non-reversing heat flow (NR) are displayed. As expected, the total heat flow shows both the step-change in heat flow at  $T_g$  and the enthalpy relaxation, the reversing signal displays only the  $T_g$  while the enthalpy relaxation appears only in the non-reversing curve.  $\Delta H_{\text{relax}}$  can thus be determined from the non-reversing heat flow and results are reported in Table S2 for all aged samples.

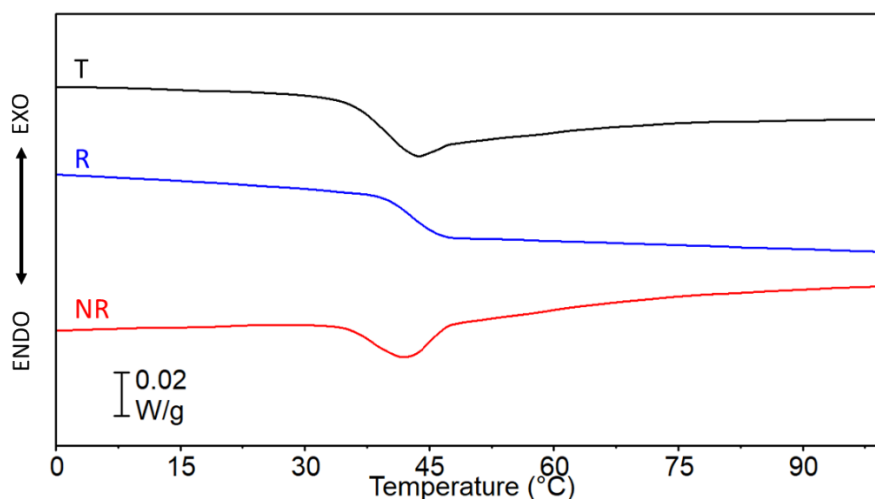


**Figure S2.** Representative MDSC analysis showing the total heat flow (black), the reversing heat flow (blue) and the non-reversing heat flow (red).

**Table S2.** Enthalpy relaxation values ( $\Delta H_{\text{relax}}$ ) determined from the non-reversing signal of MDSC for all aged samples.

Sample	Aging time [hours]	$\Delta H_{\text{relax}}$ [J/g]
PS + A6Me	0	-0.28
	24	2.27
	72	2.77
	168	3.14
PLA + A6Me	0	-0.32
	24	2.41
	72	4.98
	168	7.00
PVAc + A6Me	0	0.25
	24	0.60
	72	0.94
	168	1.97

**Table S3.** Emission properties of A6Me in PLA before and after ageing and of pure A6Me.

Sample	$\Phi^a$	$\tau^b$ [ $\mu\text{s}$ ]	$k_r^c$ [ $\text{s}^{-1}$ ]	$k_{nr}^d$ [ $\text{s}^{-1}$ ]
PLA	0.07	22	$3.2 \times 10^3$	$4.2 \times 10^4$
PLA aged (168h)	0.1	25.5	$3.9 \times 10^3$	$3.5 \times 10^4$
A6Me	1.0	3	$3.3 \times 10^5$	0

<sup>a</sup>photoluminescence quantum yield.

<sup>b</sup>lifetime.

<sup>c</sup>radiative constant.

<sup>d</sup>non-radiative constant.

### Oxygen effect during lifetime measurements

To investigate the effect of oxygen during the changes of polymer matrix we record lifetimes in air-equilibrated and under  $\text{N}_2$  atmosphere at different aging times.

Based on the equation:

$$\tau = \frac{1}{\sum k + k_q[\text{O}_2]}$$

Where  $\sum k$  is the sum of all the deactivation process of the excited state T1 of A6Me,  $k_q[\text{O}_2]$  is the quenching by oxygen.

The term  $\sum k$  is constant for a precise aging time while we could estimate  $k_q [O_2]$  by differences of the reverse of the lifetime in air-equilibrated and under  $N_2$  atmosphere. The value we calculated are  $k_q [O_2] = 6500 \text{ s}^{-1}$  for low aging time (1 hours) and  $k_q [O_2] = 6200 \text{ s}^{-1}$  for long aging time (6 months), differences lower than 5%. Variation of value of  $k_{nr}$  and  $k_r$  could be estimated with the same process and after aging these variations are  $13000 \text{ s}^{-1}$ , a value two times higher than the overall effect of oxygen and 40 times higher compared to the differences of  $k_q [O_2]$  at low aging and long aging times. Based on these data we could say that the effect of  $O_2$  is negligible compared to the effect of matrix changes.

### Mechanical characterization of polymeric films

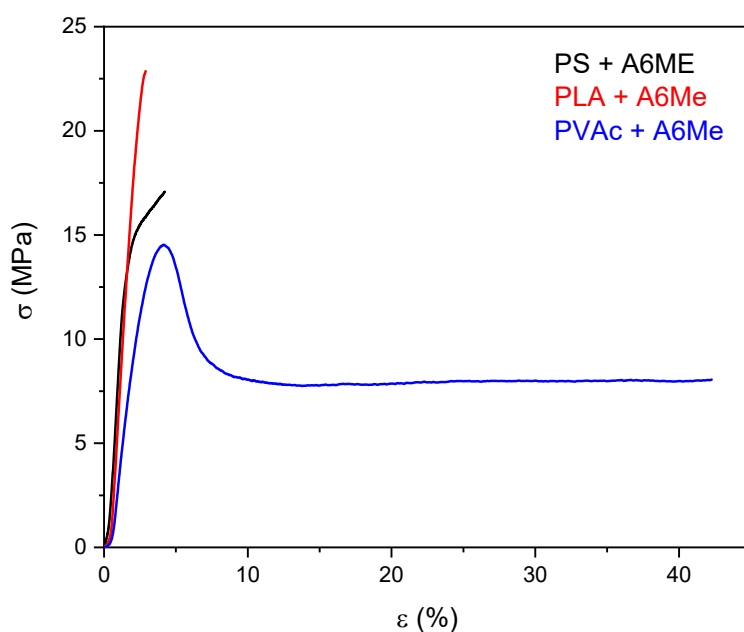


**Figure S3.** Representative stress-strain curves of A6Me doped films: PS (black), PLA (red) and PVAc (blue).

**Table S4.** Mechanical data of doped polymers (E = Young's modulus obtained from the slope of the elastic range;  $\epsilon_b$  = strain at break;  $\sigma_b$  = stress at break). Values are reported with standard deviations. Comparison between groups was performed using the one-way ANOVA and differences were considered significant for  $p < 0.05$ .

<b>Sample</b>	<b>E [MPa]</b>	<b><math>\epsilon_b</math> [%]</b>	<b><math>\sigma_b</math> [MPa]</b>
PS + A6Me	1030 ± 100	3.4 ± 0.8	16 ± 2
PLA + A6Me	1280 ± 130	3.4 ± 0.8	29 ± 6
PVAc + A6Me	660 ± 60	63 ± 17	10 ± 2
PS	1490 ± 90	2.5 ± 0.1	32 ± 4
PLA	1190 ± 90	5.5 ± 1.7	35 ± 12
PVAc	730 ± 160	77 ± 4	12 ± 4

Young's modulus, E: PS vs PS + A6Me  $p < 0.05$ ; PLA vs PLA + A6Me  $p > 0.05$ ; PVAc vs PVAc + A6Me  $p > 0.05$ .  
strain at break,  $\epsilon_b$ : PS vs PS + A6Me  $p > 0.05$ ; PLA vs PLA + A6Me  $p > 0.05$ ; PVAc vs PVAc + A6Me  $p > 0.05$ .  
stress at break,  $\sigma_b$ : PS vs PS + A6Me  $p > 0.05$ ; PLA vs PLA + A6Me  $p > 0.05$ ; PVAc vs PVAc + A6Me  $p > 0.05$ .

### **Lifetime fitting in *in situ* mechanical tests**

Lifetime values obtained during the stress-strain analysis are shown in Figure S5 (black curve) and are reported together with the stress-strain profile of the analyzed polymer (blue curve). The fitting curve of lifetime data is reported in red and the fitting function and corresponding parameters are reported in Table S4, including the standard error.

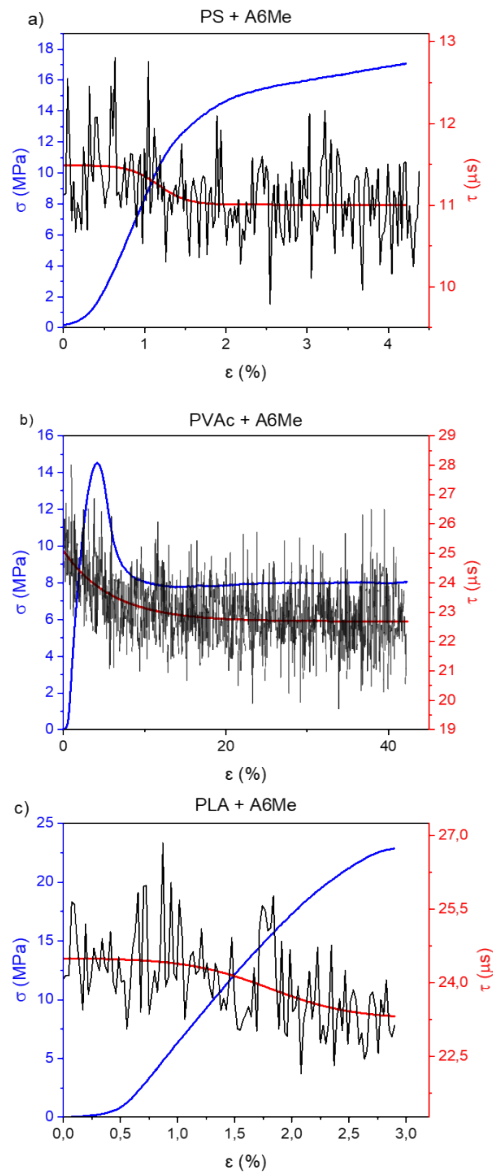


**Figure S4.** Lifetime decay of Hexakis(4-methyl-1-phenylthio)benzene, raw data (black), fitting curve (red), and stress-strain curve (blue): a) PS; b) PVAc; c) PLA.

**Table S5.** Schematic representation of the fitting function used to describe the behaviour of the Hexakis(4-methyl-1-phenylthio)benzene lifetime in the composite system during the stress-strain analysis .

Sample	Fitting function	y <sub>0</sub> [μs]	Standard Error of estimate
PVAc	Sigmoidal 5 parameters <sup>a</sup>	22.68	1.06
PS	Sigmoidal 4 parameters <sup>b</sup>	11.01	0.51
PLLA	//	23.26	0.82

$$^a f=y_0+a/(1+\exp(-(x-x_0)/b))^c ; ^b f= y_0+a/(1+\exp(-(x-x_0)/b))$$

**[Parameters]**

$$a = \max(y)-\min(y)$$

$$b=*\text{xwtr}(x,y-\min(y),.5)/4$$

$$c= 1$$

$$x_0 =**\text{x50}(x,y-\min(y),.5)$$

$$y_0 = \min(y)$$

\* xwtr. This function returns x75-x25 for sigmoidal shaped function.

\*\* This function returns the x value for the y value 50% of the distance from the minimum to the maximum of smoothed data for sigmoidal shaped. Same for x75 and x25 that returns for the y value 25% and 75% respectively of the distance from the minimum to the maximum of smoothed data for sigmoidal shaped.

## Bibliography

- [1] A. Fermi, G. Bergamini, R. Peresutti, E. Marchi, M. Roy, P. Ceroni, M. Gingras, *Dye. Pigment.* **2014**, *110*, 113.
- [2] L. C. Thomas, Modulated DSC Paper #5 - Measurement of Glass Transitions and Enthalpic Recovery (TP 010).
- [3] J. C. de Mello, H. F. Wittmann, R. H. Friend, *Advanced Materials* 1997, *9*, 230-232.]